Functional magnetic ferrogels: From biosensors to regenerative medicine

Cite as: AIP Advances **10**, 125128 (2020); https://doi.org/10.1063/9.0000021
Submitted: 06 October 2020 • Accepted: 18 November 2020 • Published Online: 30 December 2020

G. V. Kurlyandskaya, F. A. Blyakhman, E. B. Makarova, et al.

Functional magnetic ferrogels: From biosensors to regenerative medicine

Cite as: AIP Advances 10, 125128 (2020); doi: 10.1063/9.0000021
Presented: 4 November 2019 • Submitted: 6 October 2020 •
Accepted: 18 November 2020 • Published Online: 30 December 2020

G. V. Kurlyandskaya,[1,2,a)] F. A. Blyakhman,[2,3] E. B. Makarova,[3,4] N. A. Buznikov,[5] A. P. Safronov,[2,6] F. A. Fadeyev,[3] S. V. Shcherbinin,[2,6] and A. A. Chlenova[2,7]

AFFILIATIONS

[1]Department Electricity and Electronics, Basque Country University U4PV-EHU, 48940 Leioa, Spain
[2]Ural Federal University, 620002 Ekaterinburg, RF
[3]Ural State Medical University, 620028 Ekaterinburg, RF
[4]Ural Scientific Institute of Traumatology and Orthopedics, 620014 Ekaterinburg, RF
[5]Scientific and Research Institute of Natural Gases and Gas Technologies, 142717 Moscow, RF
[6]Institute of Electrophysics, UD RAS, 620016 Ekaterinburg, RF
[7]Institute of Metal Physics, UD RAS, 620108 Ekaterinburg, RF

Note: This paper was presented at the 65th Annual Conference on Magnetism and Magnetic Materials.
[a)]**Author to whom correspondence should be addressed:** kurlyandskaya@gmail.com

ABSTRACT

Polyelectrolyte gels and ferrogels (FG) are attracting special interest in biomedicine. Here we describe our experience developing functional magnetic ferrogels for regenerative medicine and magnetoimpedance biosensing for measuring stray fields of nanoparticles in FG with a multilayered sensitive element. We discuss the possibility of developing a new generation of drug delivery systems for magnetic field assisted delivery, positioning and biosensing.

I. INTRODUCTION

A hydrogel is a solution (typically in water) of flexible polymer chains bonded to each other in a finite number of points. They form a 3D cross-linked polymeric network with chain sections between crosslinks containing above 50 monomer units. If the polymer chains carry an electric charge, the gel is denominated "polyelectrolyte" – an equivalent number of oppositely charged counter ions corresponds to the gel medium.[1,2] The physical properties of a gel are similar to the solution of a polymer in a liquid. There is a difference, however: a gel retains its shape and has elasticity. A significant increase in the deformation level under the application of a magnetic field can be achieved for magnetic ferrogel (FG), i.e. a multicomponent system, consisting of magnetic nanoparticles (MNPs) spread over polymeric network swollen in liquid.[3] FG can be prepared by incorporating magnetic nanoparticles or even magnetic wires into chemically cross-linked hydrogels.[4–6] Nowadays a large variety of FG can be synthesized. Fig. 1 shows some typical examples.

There are different reasons for the interest in biomedical applications of gels and ferrogels. Polyelectrolyte gels and FG are attracting special interest in the area as biomimetic materials. Many features of biological tissues vary from one biological system to another especially in the case of tumor tissues.[7] At the first stage of many biomedical studies, the substitution of biological samples by synthetic hydrogels or FG to mimic the main properties of living tissues makes sense. Synthetic hydrogels can be used as simplified models of the cytoskeleton and in addition do not require a strict protocol for testing and safekeeping.

Fig. 2 summarizes some selected prospects for the practical use of ferrogels: controlled drug release, biocompatible valves and actuators controlled by a magnetic field, magnetic biosensors, matrices for growing cells and tissues including conditions of growing in a magnetic field. Recently, we reported on the possibility of

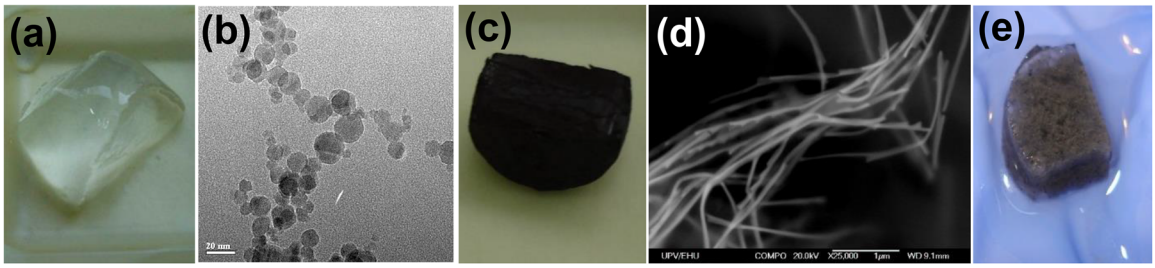

FIG. 1. General view of hydrogel (a). Transmission electron microscopy of iron oxide MNPs obtained by laser target evaporation technique (LTE) (b) and general view of FG with 2.4% by weight of iron oxide LTE MNPs (c). Scanning electron microscopy of nickel nanowires synthesized by electrodeposition into commercial anodic aluminum oxide templates with an 80 nm pore diameter (d) and general view of FG with nickel nanowires (e).

cultivating human dermal fibroblast cell cultures,[8] which also might be useful for regenerative medicine. As in previous tests with magnetic biosensing systems, polyacrylamide-based FG with embedded magnetic nanoparticles of iron oxide were used for cultivating human dermal fibroblast cell cultures. Biocompatible γ-Fe_2O_3 MNPs were obtained by the laser target evaporation technique (LTE),[9] which provides large batches greatly requested in nanomedicine.[7] The above-mentioned approach of cell cultivation onto gel/FG surfaces might be useful for regenerative medicine, drug delivery and biosensor applications opening a new combination of magnetic field assisted delivery, positioning control and post operation monitoring. In-tissue embedded MNP detection is one of the most sought-after biomedical applications. In previous publications we reported on a magnetic biosensor prototype with a magnetic multilayered sensitive element for the detection of mesoscopic distributions of nanoparticles using the magnetoimpedance (MI) effect.[10] MI responses were measured with and without a polyacrylamide FG layer in order to evaluate stray fields of embedded MNPs. For the development of a new generation of drug delivery systems for multifunctional devices a further increase of the sensitivity of the magnetic field sensor is necessary.

In this work, we describe our experience developing functional magnetic polyacrylamide ferrogels with examples in the field of regenerative medicine and magnetic biosensing using iron oxide γ-Fe_2O_3 magnetic nanoparticles produced by LTE.

II. EXPERIMENTAL PROCEDURE, MATERIALS AND METHODS

Iron oxide MNPs were prepared by the LTE method (more details of their characterization can be found elsewhere[11]). Polyacrylamide (PAAm) FG with a network density of 1:100 were synthesized by radical polymerization of acrylamide in a stable aqueous suspension of iron oxide MNPs. Concentrations of 2.4%, 2.1%, 1.3% and 1.0% of MNPs by weight were obtained. More details about the FG preparations can be found elsewhere.[9] Magnetoactive epoxy composites with particles (Alfa Aesar) characterized by a unimodal lognormal size distribution with a median of 250 nm were used as a magnetic filler for additional testing of the MI sensor prototype. The saturation magnetization of magnetite particles was 84 emu/g. Composites containing 5, 10, 30, 50, 70 (wt. %) were synthesized.

In experiments in-vitro, the FG biocompatibility was estimated by the proliferation rate of chondrocytes after 4 days of incubation. A primary culture of chondrocytes was obtained from the cartilage tissue of a sexually mature Wistar rat following the standard procedure[11] with the use of a Human Chondrocyte Growth Medium Kit (Cell applications, Inc, USA). 8 samples of PAAm gels and 8 samples of PAAm FG in the shape of disks (diameter ~13 mm, 1mm thick) were placed into the wells of a polystyrene plate (Techno Plastic Products, Switzerland). A chondrocytes suspension in a growth medium was dispensed into all plate wells with a seeding density of 3000 viable cells/cm.[2] The plate with cells was incubated in a CO_2

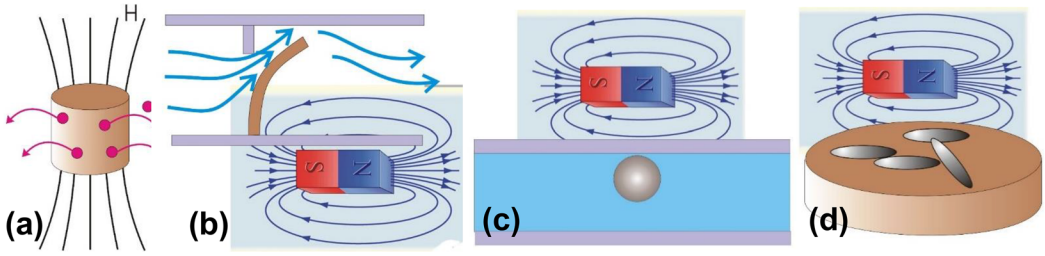

FIG. 2. Prospects for the practical use of ferrogels. Controlled drug release (a). Biocompatible valves and actuators controlled by a magnetic field (b). Magnetic biosensors (c). Matrices for growing cells and tissues including conditions of growing in a magnetic field (d).

incubator for 4 days, and the cell monolayer density was calculated after that. In the experiments with animals, the PAAm FG with 1.3 wt. % of MNPs concentration were examined. All animal experiments were performed in accordance with the International Guiding Principles for Biomedical Research Involving Animals (CIOMS, 1985) and approved by the Ethics Committee of the Ural State Medical University (Record #2 on Feb'28, 2020).

The multilayered elements for the biosensor were deposited by dc-sputtering with the application of an external magnetic field along the short side of the rectangular 10× 0.5 (mm^2) element. FeNi/Ti and FeNi/Cu based structures were considered. The MI was measured in the "microstripe" line.[10] The MI ratio for the impedance Z was calculated as follows: $\Delta Z=[Z(H)-Z\ (H_{max})]/Z\ (H_{max})$, H_{max} = 100 Oe. The magnetization curves were measured by a vibrating sample magnetometer. To analyze the MI effect in multilayers we proposed an electrodynamic model.[12] Since the multilayer length and width are much higher than its thickness, the field distribution within the layers can be found in the one-dimensional approximation by means of a solution of linearized Maxwell equations. To describe the field distribution outside the multilayer we use the approximate solution for the vector potential obtained previously.[13] The MI response was found by taking into account the continuity conditions for the electric and magnetic fields at the interfaces between layers and at the multilayer surface.

III. RESULTS AND DISCUSSION

A. Biological testing

The following cell counts after incubation were obtained for PAAm gel (control 1), PAAm + γ-Fe_2O_3 and polystyrene (control 2): 180 ± 60, 1500 ± 600 and 23500 ± 1800 cells/cm,[2] respectively. The data is presented in the form $X \pm m$, where m is the standard error of the arithmetic average X, n = 72 (9 fields of view per well × 8 wells). The results obtained imply that the addition of MNPs to the network of PAAm gel results in a significant increase of the cell proliferation rate. Thus, the FG biocompatibility estimated by monolayer density of chondrocytes after 4 days of culturing is much higher than in the blank gel and closer to the tissue culture polystyrene. Qualitatively the same results were reported early with respect to human dermal fibroblasts.[8]

In vivo experiments were performed with 6 sexually mature male rabbits "Soviet Chinchilla" (certificate No. 2020/2KSh dated April 12, 2020), one of which was used as a donor for chondrocytes. During the surgery of the five animals, cylindrical osteochondral defects (5 mm in diameter and 5.5 mm in length) were formed on the anterior surface of the distal epimetaphysis femur of both limbs. Unsubstituted defects (4 defects) were the control for assessing the response of the surrounding tissues to surgery. PAAm-Fe_2O_3 (2 implants) and PAAm-Fe_2O_3 with allogeneic chondrocytes applied to the surface of the implant (4 implants) were tested. The cells were isolated from cartilage tissue and cultured using standard methods.[14] The animals were taken out of the experiment 30 days after the day of operation. The defect area and adjacent bone and cartilage tissue of the host bone bed were examined by morphological and morphometric methods (Fig. 3). The biocompatibility was evaluated by the semi-quantitative assessment of the local biological effect of implants[14] based on the determination of the presence of necrotic zones, counting the number of pro-inflammatory cells – polymorphonuclear leukocytes, lymphocytes, macrophages, plasma cells and giant multinucleated cells.

It was found (Fig. 4) that the introduction of implants (PAAm-Fe_2O_3 and PAAm-Fe_2O_3-allogeneic chondrocytes) caused the development of small necrotic foci in the adjacent tissues (in 3 out of 6 cases), activation of lymphocytes and macrophages. As expected, there was a tendency to an increase in the intensity of the local inflammatory reaction. An increase in the number of lymphocytes and macrophages in the maternal bed tissues was observed after the introduction of PAAm-Fe_2O_3-allogeneic chondrocytes in comparison with the control and the PAAm-Fe_2O_3. However, the severity of the signs of local inflammatory reaction did not significantly differ from control ($p \leq 0.1$). There were no signs of rejection or severe degradation of the implant during the introduction of both types of implants – there were no giant multinucleated cells, the number of neutrophils increased insignificantly compared to the control. Thus, under present conditions and taking into account the overall assessment of the selected criteria, the PAAm-Fe_2O_3 can be considered as a relatively inert[15] or a biotolerant material.[16]

B. MI effect in multilayered structures and FG testing

Coming back to the idea of combining positioning control and post operation monitoring for *in vivo* experiments with replacement of cartilage, we propose to develop an MI sensor for the detection of stray fields of MNPs of a FG implant. Fig. 5 shows an example of the characterization of multilayers, experimental frequency and field dependences of MI, including a FG detection example.

The MI effect in multilayers is governed by changes in the skin depth with the transverse permeability of FeNi layers. To find the transverse permeability we assume that FeNi layers have a uniaxial

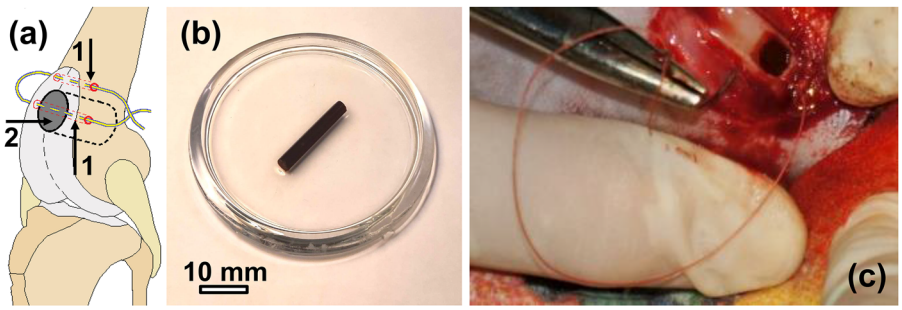

FIG. 3. (a) Operation scheme: 1 – two transverse channels for fixing the implant to the defect walls with a transosseous suture, 2 – cylindrical osteochondral defect with implant; (b) FG sample from which the implants were cut (diameter 5 mm); (c) fixation with the transosseous suture of the FG implant to the walls of the defect of the rabbit femur epimetaphysis.

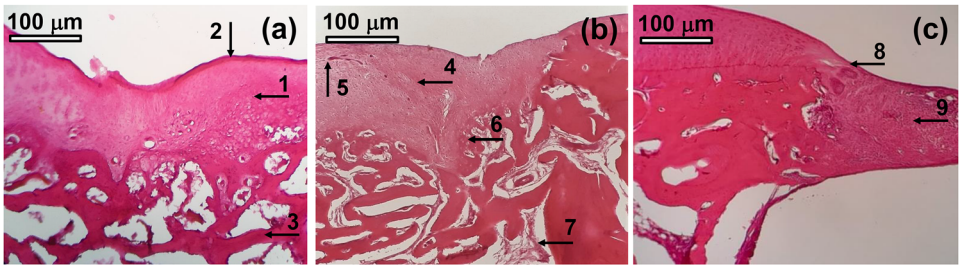

FIG. 4. Histological preparations of the distal articular surface of the femur of the rabbit. The boundaries of the defect areas are the host bone bed (staining by hematoxylin and eosin). Control (a): 1 – the articular surface of the regenerate is represented by a wide layer of newly formed hyaline-fibrous cartilage tissue, covered with the perichondrium – 2; trabeculae of cancellous bone tissue – 3. PAAm-Fe_2O_3 implant (b): from the articular surface, the defect is covered with dense fibrous connective tissue with many fibroblastic cells – 4; the intercellular substance is permeated with small capillaries – 5; the foci of chondrogenesis are defined in the form of roller-like thickenings at the cartilage-defect border and in the geometry of plates in the inner layer of the perichondrium covering the defect area – 6; the cells of the hyaline-like cartilage tissue are large and poorly differentiated; red bone marrow – 7. Implant PAAm-Fe_2O_3-allogeneic chondrocytes (c): the marginal zone of the cartilage-defect border contains fine-fibrous structures – 8; islets of cells formed by fibroblast-like cells and single chondrocytes –9.

in-plane magnetic anisotropy, and the anisotropy field (H_a) and angle of deviation of the anisotropy axis from the transverse direction are the same for all FeNi layers. The transverse permeability of FeNi layers is obtained from a solution of the Landau–Lifshitz equation neglecting the contribution of the domain-walls motion. The developed model allows one to analyze the influence of multilayer parameters on the MI effect. Fig. 6(a) shows a calculated frequency dependence of the maximum MI ratio $(\Delta Z/Z)_{max}$. The parameters of the FeNi layers used for calculations are: saturation magnetization M=750G, H_a=6Oe, anisotropy axis angle $\psi=0.1\pi$, conductivity $\sigma=3\times10^{16}s^{-1}$, and the Gilbert damping parameter κ=0.02. It follows from Fig. 6(a) that the value of $(\Delta Z/Z)_{max}$ decreases with the magnetic layer thickness. Furthermore, the MI effect increases when the conductivity of the spacers decreases (we assume that Cu conductivity $\sigma_{Cu}=5\times10^{17}s^{-1}$ and Ti conductivity $\sigma_{Ti}=5\times10^{16}s^{-1}$). The analysis demonstrated that the MI maximum can be achieved when the spacer conductivity becomes comparable in magnitude with the FeNi conductivity.[17] It was found also that the further enhancement of the MI can be obtained in multilayers with thinner spacers and by using magnetic materials for spacers.[18] The increase of $(\Delta Z/Z)_{max}$ in the multilayers with magnetic spacers is due to the fact that the difference between the skin depths in the spacers and in the FeNi layers is less pronounced: the field distribution within the multilayer becomes more uniform, leading to the MI increase (Fig.6). The presence of FG changes the field distribution within multilayered film structure and correspondingly affects the MI response. A model for the MI effect in multilayers with FG was developed recently.[10] In accordance with the model, the FG layer has a double effect on the MI response. The first contribution to the MI effect is attributed to the high permittivity of the FG layer, which results in an increase of the MI in the multilayer with FG. The second contribution of the FG comes from stray fields of MNPs.

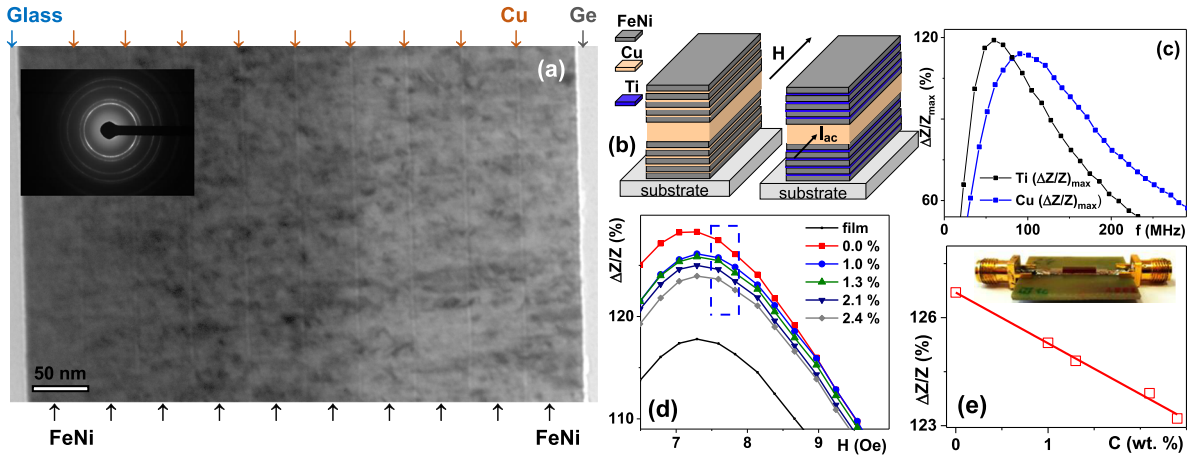

FIG. 5. Transmission electron microscopy for [Cu(3 nm)/FeNi(50 nm)]$_{10}$ multilayer with well resolved periodic structure; inset shows microdiffraction data (a). General structure of FeNi/Ti and FeNi/Cu MI multilayers (b). Experimental frequency dependences of the maximum of MI ratio $(\Delta Z/Z)_{max}$ for FeNi/Cu and FeNi/Ti MI multilayers (c). Experimental results for FG detection: work interval is framed by blue dashed line (d). Measured concentration dependence of MNPs in FG for 100 MHz frequency in the field of about 8 Oe; photo shows FG sample on top of FeNi/Cu element in the "microstripe" line (e).

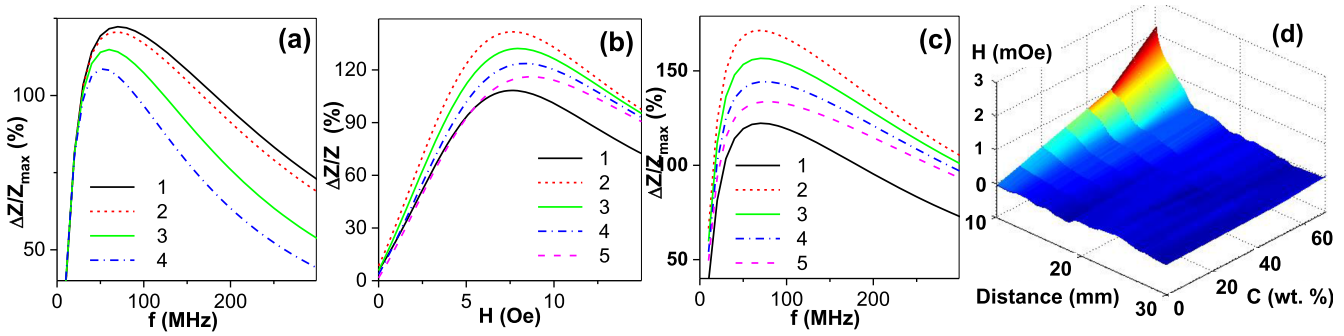

FIG. 6. Calculated frequency dependence $(\Delta Z/Z)_{max}$ for MI structures: 1 – $[Ti/FeNi(100)]_5/Ti/Cu(500)/Ti/[FeNi(100)/Ti]_5$; 2 – $[Ti/FeNi(50)]_{10}/Ti/Cu(500)/Ti/[FeNi(50)/Ti]_{10}$; 3 – $[Cu/FeNi(100)]_5/Cu(500)/[FeNi(100)/Cu]_5$; 4 – $[Cu/FeNi(50)]_{10}/Cu(500)/[FeNi(50)/Cu]_{10}$ (a). Calculated MI ratio as a function of the field at f=150MHz (b) and the MI maximum frequency dependence (c): 1 – $[Ti/FeNi(100)]_5/Ti/Cu(500)/Ti/[FeNi(100)/Ti]_5$; 2 – H_p=0; 3 – H_p=0.25Oe; 4 – H_p=0.5Oe; 5 – H_p=0.75Oe. Dependence of the detector signal level on the concentration of magnetite particles in the epoxy composites at different distances (d).

To describe qualitatively the effect of stray fields on the MI response, it is supposed that the FG layer induces a spatially homogeneous effective stray field H_p. The value of H_p is assumed to be proportional to the concentration of MNPs in the ferrogel.[10] The field dependence of the MI ratio calculated at 150MHz for $[Ti(6)/FeNi(100)]_5/Ti(6)/Cu(500)/Ti(6)/[FeNi(100)/Ti(6)]_5$ structure (curve 1) and the multilayer with FG for different values of the effective stray field H_p (curves 2–5) is shown in Fig. 6(b). The frequency dependence of the maximum MI ratio $(\Delta Z/Z)_{max}$ for the same samples is shown in Fig. 6(c). In the presence of the gel without MNPs (H_p=0), the MI increases due to high permittivity of the gel. The effective stray field H_p increases with the concentration of magnetic nanoparticles in the FG, and the MI ratio decreases with an increase of H_p. The calculated dependences are in a qualitative agreement with experimental results (Fig. 5(d)). The stray fields change the magnetization distribution in the FeNi layers and affect the multilayer permeability allowing to measure the MNPs concentration in FG (Fig. 5(e)). As the next step to develop a magnetic biosensor for regenerative medicine purposes, we designed a scanning system to monitor the position and state of a FG implant at a distance. The first measurements of concentration dependence were made for the cylindrical samples of epoxy composites with commercial magnetite particles (Fig. 6(d)).

IV. CONCLUSIONS

We described our experiments in the development of polyacrylamide ferrogels with γ-Fe_2O_3 magnetic nanoparticles produced by LTE. The examples provided in the field of regenerative medicine for cartilage replacement and magnetic biosensing using FeNi/Ti and FeNi/Cu based MI multilayers confirm the capacity of these functional materials for biomedical applications.

ACKNOWLEDGMENTS

This work was supported by the RSF project 18-19-00090. We thank O.M. Samatov, B. Stadler, V.N. Lepalovskij, M.A. Korch, A.V. Svalov, D.G. Blisnets, A. Larrañaga, I. Orue, and M.N. Volochaev for support. Selected measurements were made at SGIKER UPV/EHU.

DATA AVAILABILITY

The data that support the findings of this study are available from the corresponding author upon reasonable request.

REFERENCES

[1] P. C. Hiemenz and R. Rajagopalan, *Principles of Colloid and Surface Chemistry* (Marcel Dekker, New York, NY, USA, 1997).
[2] M. Zrínyi, L. Barsi, and A. Büki, Polym. Gels Networks **5**, 415 (1997).
[3] J. A. Galicia, F. Cousin, E. Dubois, O. Sandre, V. Cabuil, and R. Perzynski, J. Magn. Magn. Mater. **323**, 1211 (2011).
[4] F. Blyakhman, E. Makarova, F. Fadeyev, D. Lugovets, A. Safronov, P. Shabadrov, T. Shklyar, G. Melnikov, I. Orue, and G. Kurlyandskaya, Nanomaterials **9**, 232 (2019).
[5] P. Bender, A. Günther, A. Tschöpe, and R. Birringer, J. Magn. Magn. Mater. **323**, 2055 (2011).
[6] A. P. Safronov, B. J. H. Stadler, J. Um, M. R. Zamani Kouhpanji, J. Alonso Masa, A. G. Galyas, and G. V. Kurlyandskaya, Materials **12**, 2582 (2019).
[7] J. H. Grossman and S. E. McNeil, Phys. Today **65**, 38 (2012).
[8] F. A. Blyakhman, G. Y. Melnikov, E. B. Makarova, F. A. Fadeyev, D. V. Sedneva-Lugovets, P. A. Shabadrov, S. O. Volchkov, K. R. Mekhdieva, A. P. Safronov, S. Fernández Armas, and G. V. Kurlyandskaya, Nanomaterials **10**, 1697 (2020).
[9] A. P. Safronov, I. V. Beketov, S. V. Komogortsev, G. V. Kurlyandskaya, A. I. Medvedev, D. V. Leiman, A. Larrañaga, and S. M. Bhagat, AIP Advances **3**, 052135 (2013).
[10] N. A. Buznikov, A. P. Safronov, I. Orue, E. V. Golubeva, V. N. Lepalovskij, A. V. Svalov, A. A. Chlenova, and G. V. Kurlyandskaya, Biosens. Bioelectron. **117**, 366 (2018).
[11] M. Gosset, F. Berenbaum, S. Thirion, and C. Jacques, Nat. Protoc. **3**, 1253 (2008).
[12] N. A. Buznikov and G. V. Kurlyandskaya, Sensors **19**, 1761 (2019).
[13] A. Gromov, V. Korenivski, D. Haviland, and R. B. van Dover, J. Appl. Phys. **85**, 5202 (1999).
[14] Interstate Standard ISO 10993-6-2011: «Medical Devices. Biological Evaluation of Medical Devices. Part 6. Tests for Local Effects after Implantation».
[15] L. L. Hench and J. R. J. Biomaterials, *Artificial Organs and Tissue Engineering* (CRC PressWoodhead, Boca Raton, Cambridge, 2005), p. 304.
[16] M. Zborowski and J. Chalmers, *Magnetic Cell Separation* (Elsevier, 2008), p. 486.
[17] N. A. Buznikov and G. V. Kurlyandskaya, J. Phys.: Conf. Ser. **1389**, 012132 (2019).
[18] A. V. Svalov, E. Fernandez, A. Garcia-Arribas, J. Alonso, M. L. Fdez-Gubieda, and G. V. Kurlyandskaya, Appl. Phys. Lett. **100**, 162410 (2012).